

EVOLUTION OF PLASTIC DEFORMATION AND TEMPERATURE AT THE REFLECTION OF A SHOCK PULSE FROM SUPERFICIES WITH A NANORELIEF OR WITH SUPPLIED NANOPARTICLES

A.A. Ebel, A.E. Mayer

South Ural State University, Chelyabinsk, Russian Federation

E-mail: ebela@usu.ru, mayerae@usu.ru

Intense irradiation and high-speed collision of metals results in the formation and dissemination of shock compression pulses in them. The recent development of experimental technology using high-power subpicosecond laser pulses makes it possible to obtain shock pulses of the picosecond range. A molecular dynamics simulation of high-speed collisions for aluminium samples is conducted. The presence of a nanorelief or precipitated nanoparticles on the back surfaces of the sample may essentially enhance the rear splitting threshold. The cooperation of a shock wave with a nanorelief or precipitated nanoparticles results in strong plastic deformation. Consequently, part of the compression pulse energy is spent on plastic deformation, which prevents spall destruction. The effect of increasing the threshold can reach hundreds of meters per second in terms of collision speed and tens of gigapascals in amplitude of the incident shock wave. The distribution of shear strain and temperature in the sample is considered. It is shown that the maximum degree of deformation and maximum heating are observed in those parts of the nanorelief, for which the greatest change in shape is observed. The maximum temperature reaches the melting point, but no obvious traces of melting are found, which may be related to the speed of the processes.

Keywords: high speed impact; plastic deformation; molecular dynamics; nanorelief.

Introduction

High-speed collision [1, 2] and intense irradiation [3, 4] of metals results in the formation and dissemination of shock compression pulses in them. The recent development of experimental technology using high-power sub-picosecond laser pulses makes it possible to obtain shock pulses of the picosecond range [2, 4, 5]. The method of molecular dynamics (MD) is often used in the theoretical study of the phenomenon of broken fragments. At the same time the study of the behavior of the nanometric zones of metals in the conditions of the model train [6–10] and the direct modeling of the formation and the elimination of shock waves triggered by a piston or a hammer [6, 11–16]. Despite the fact that only relatively small system volumes and process times can be considered due to technical restrictions, MD modeling offers several advantages. It offers the possibility of automatically taking into account the evolution of the structure of the material during high speed forming, at least qualitatively. The accuracy of the quantitative description is determined by the quality of the interatomic potentials used.

Practically important is the question of the stability of the material to rear fragmentation and the intensity of the threshold of the incident shock wave or the speed of impact of the threshold at which fragmentation will occur. The fragmentation threshold is determined by two factors: (i) the resistance of the material to tensile stresses; (ii) the relationship between the amplitude of the incident compression pulse and the amplitude of the expansion pulse reflected from the free surface. The tensile strength of metals was carefully studied by modeling [6–9, 11–16], including the effect of [6–8], cavities [9, 12, 16], grain boundaries [12–14], twins [15] inclusions. Also noteworthy is the problem of reducing the amplitude of the tensile wave that forms on the free surface.

If the free surface is not flat and has protrusions or grooves, the uniaxial deformed state performed in a plane shock wave will be replaced by a more complex deformed state when interacting with these relief elements. For example, when a shock wave enters cylindrical protrusions on the rear surface of the target, a discharge on the lateral surfaces of the cylinders leads to a transition to a state of uniaxial tension. As a result, compressive and tensile stresses are limited by the dynamic yield strength. The process of interaction of the incident shock wave with the protrusions leads to intense plastic de-

plastic deformation in the superfcy layer, as a result of which part of the energy of the compression pulse is scattered. This should lead to a decrease in the amplitude of the expansion wave and, consequently, to an increase in the fragmentation threshold. A significant effect should be expected when the size of the reliefs or other elements in the relief are comparable to the width of the compression pulse. If the width of the compression pulse is much larger than the height of the protrusions or if the shock wave is strong enough, the allowed plastic deformation of the protrusions becomes insufficient to effectively suppress the reflected wave. The presence of protrusions in this case can lead to the development of Richtmyer–Mashkov instability and to release [17–19] jets, as in the case of liquids. Work is underway on modeling MD ejection stream from nanostructured metal superficite, initiated by sufficiently strong shock waves [18, 19]. At the same time, there are no MD studies regarding the effect of dorsal superfica relief on the scaling threshold. Also of interest is the investigation with MD with a similar effect in the presence of a layer of precipitated nanoparticles on a flat superficy. This article deals with the analysis of this effect. The development of the plastic deformation and temperature is considered after the reflection of an impact compression pulse from the superficy with nanorelief and with deposited nanoparticles.

1. Problem Statement

The molecular dynamic systems of samples from single-crystalline aluminum are considered. The direction of the x , y and z axes is chosen by the crystallographic directions [100], [010], and [001]. After initial thermalization for 2 ps in a thermostat at 300 K and in a barostat at zero pressure, the flat, superficial layer of thickness H (15 or 30 grating periods) received an additional velocity v , which along the x -axis was normal to the boundary with the x was directed to rest of the system (Fig. 1) [20]. The lateral dimensions of the system were 30 lattice periods. The additional velocity was added to the thermal velocity of each atom of this flat layer that played the role of a drummer. Either a cylindrical projection with a height of l and a diameter d or precipitated particles with a common layer thickness of l and different diameters d were set on the rear superficy of the target. The height l of the cylinder or the thickness of the layer of particles varied from 0, which corresponds to a flat back ultrafast, up to 60 lattice parameters. The diameter d of the cylindrical protrusion or deposited nanoparticles also varied from 14 to 30 lattice periods. Note that we compared the strength of the samples with the same total thickness L , which includes the height of the protrusion or of the deposited particles.

Molecular dynamics modeling was carried out using LAMMPS [21]. The calculations were made for aluminum using the interatomic potential [22]. Both potentials are based on the method of immersed atoms. The atomic configurations were visualized using the OVITO [23] program. The fault structure was visualized on the basis of a central symmetry parameter [24], which is zero for an ideal fcc network, and the difference of zero shows the degree of defect; the common neighbor analysis algorithm was also used [25, 26].

To reach a state of thermodynamic equilibrium before the collision started, a barostat and a Nose-Hoover thermostat were used. After establishing the impact velocity, the calculations were made within the NVE set (the time energy E , the volume of the system V and the number of particles N are constant). Periodic boundary conditions have been specified along all axes. The calculation domain was chosen to be significantly larger than the size of the molecular dynamics system along the direction of the collision coinciding with the x axis. This ensured compliance with the conditions of the free superficy at the attacker's border and the rear superficy of the target. A finished thickness beater generated a compression pulse composed of a shock wave followed by an unloading wave. Maximum compressive stresses were determined by the impact velocity v . In the case of the presence of protrusions or deposited nanoparticles on the back superficy ($l > 0$), this is equivalent to a sample with periodically located protrusions [20, 27–29].

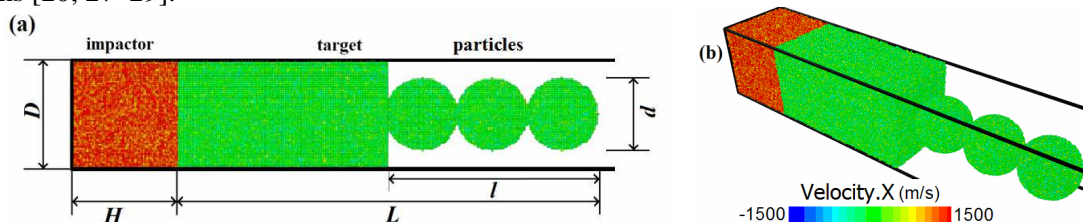


Fig. 1. Configuration of the MD system at the beginning of the collision: a) the schematic model and b) the general view, the color shows the x component of the atom velocity [20]

2. Discussion of Results

Plastic deformation, as in the macroscopic case, is defined as irreversible deformation of the material after removal of the external load. The magnitude of the deformation is calculated through the derivatives with respect to the coordinates of the displacement of atoms from the initial state. In the considered problems, the removal of the load means the departure of the wave from the region near the back superficiality. Thus, irreversibility is the main feature that allows us to distinguish plastic deformation, including in molecular dynamics calculations. An indirect sign that the deformation is plastic is the magnitude of shear deformation: shear deformations greater than 0,1–0,2 correspond to the plastic mode.

The magnitude of plastic deformation upon reflection of a shock pulse from a nanorelief superficiality is analyzed. In Fig. 2 shows, in the case of a flat boundary, the distribution of shear strain calculated from the displacement of atoms [30]. Similarly calculated and shown in Fig. 3 distribution of shear strain in the case of a cylindrical protrusion and deposited nanoparticles. The magnitude of the deformation reaches one or more, which is substantially more than the possible elastic deformations. From this it follows that the presented distributions correspond precisely to plastic deformation. In this case, the zones of plastic deformation correspond to those parts of the nanorelief that have undergone the greatest change in shape when exposed to a shock wave. Also, the deformation corresponds to the region of the sample in which a spallation is formed in the case of a flat superficiality (Fig. 2) and an incomplete spallation in the case of a nanorelief at a high impact velocity (Fig. 3).

Plastic deformation is accompanied by heating of the material. The temperature distributions calculated from the average kinetic energy of a disordered motion are shown in Fig. 4, 5 for the same time points as the deformation in Fig. 2, 3. The greatest temperature increase is observed in the most deformed parts of the nanorelief and in the spall formation zone. The maximum temperature reaches the melting point, but no obvious traces of melting are found, which may be due to the speed of the processes. At later stages, thermal conductivity has a significant effect on the temperature distribution in the sample.

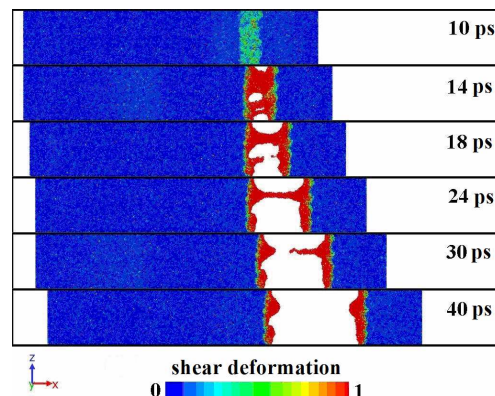


Fig. 2. Shear deformation in the central section of an aluminum target with a flat rear superficiality; when the impactor speed is 1500 m/s and the total target thickness is 120 lattice parameters (48,6 nm)

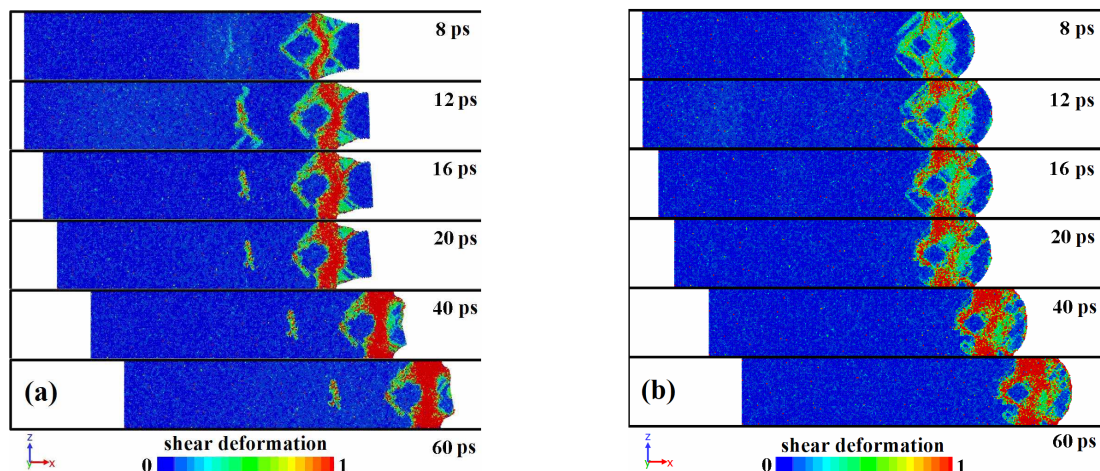


Fig. 3. Shear deformation in the central section of an aluminum target with a hammer speed of 1500 m/s and a total target thickness of 120 lattice parameters (48,6 nm): a) with cylindrical projections with $H = 1$; b) with deposited particles with $H = 1$ (diameter of 30 lattice parameters (12,15 nm), one layer)

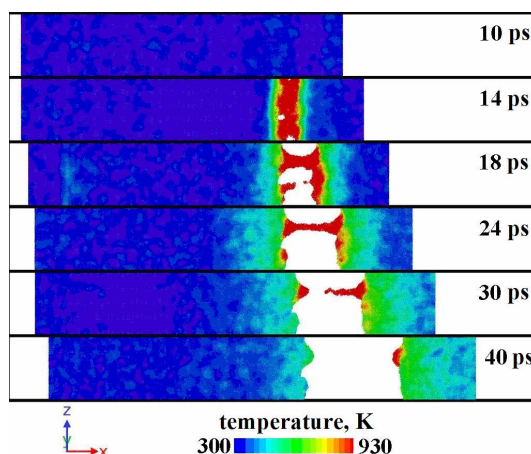


Fig. 4. The temperature in the central section of the aluminum target with a flat rear superficy; when the impactor speed is 1500 m/s and the total target thickness is 120 lattice parameters (48,6 nm)

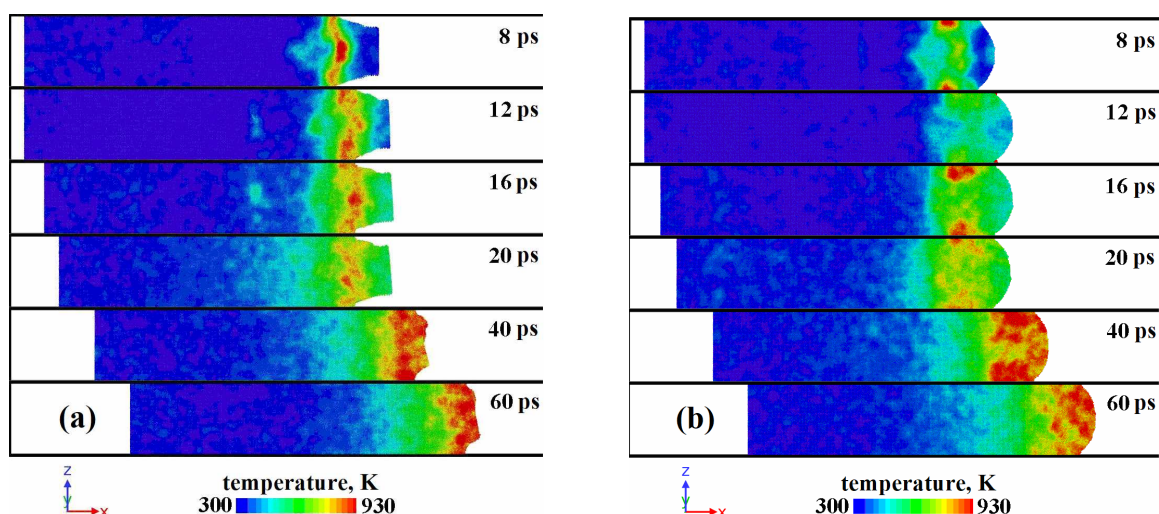


Fig. 5. The temperature in the central section of the aluminum target with a hammer speed of 1500 m/s and a total target thickness of 120 lattice parameters (48,6 nm): a) with cylindrical projections with $H/H = 1$; b) with deposited particles with $H/H = 1$ (diameter of 30 lattice parameters (12,15 nm), one layer)

Conclusion

A study of the molecular dynamics of high speed collisions for aluminum samples shows that the presence of cylindrical protuberances or nanoparticles deposited on the rear superficy of the sample can considerably increase the rear fractionation threshold. Note that the deposited nanoparticles make the free superficy more resistant to burst fracture initiated by the reflected compression pulse. The reason is that when a shock wave arrives at the rear of the superficy with protrusions, the discharge of the protrusions on the lateral superficy occurs, leading to severe plastic deformation. Consequently, part of the energy of the compression pulse is devoted to plastic deformation, which limits the amplitude of the stretching pulse and suppresses the destruction of the substance during tensile stresses. The effect of increasing the threshold can reach hundreds of meters per second in terms of collision speed and tens of gigapascals in amplitude of the incident shock wave. An analysis of the distribution of shear deformations and temperature in the sample shows that the maximum degree of deformation and maximum heating are observed in those parts of the nanorelief for which the greatest change in shape is observed. The maximum temperature reaches the melting point, but no obvious traces of melting were found, which may be related to the speed of the processes.

This work is supported by the Ministry of Science and Higher Education of Russian Federation (state assignment for researches by CSU № 075-00992-21-00) and by Act No. 211 from 16 March of 2013 of the Government of the Russian Federation (Contract No. 02.A03.21.0011).

References

1. Kanel G.I., Fortov V.E., Razorenov S.V. Shock Waves in Condensed-State Physics. *Physics Uspekhi*, 2007, Vol. 50, pp. 771–791. DOI: 10.1070/PU2007v050n08ABEH006327

2. Zaretsky E.B., Kanel G.I. Yield Stress, Polymorphic Transformation, and Spall Fracture of Shock-Loaded Iron in Various Structural States and at Various Temperatures. *Journal of Applied Physics*, 2015, Vol. 117, Iss. 19, p. 195901. DOI: 10.1063/1.4921356
3. Ashitkov S.I., Komarov P.S., Struleva E.V., Agranat M.B., Kanel G.I. Mechanical and Optical Properties of Vanadium under Shock Picosecond Loads. *JETP Letters*, 2015, Vol. 101, pp. 276–281. DOI: 10.1134/S0021364015040049
4. Gnyusov S.F., Rotshtein V.P., Mayer A.E., Rostov V.V., Gunin A.V., Khishchenko K.V., Levashov P.R. Simulation and Experimental Investigation of the Spall Fracture of 304L Stainless Steel Irradiated by a Nanosecond Relativistic High-Current Electron Beam. *International Journal of Fracture*, 2016, Vol. 199, Iss. 1, pp. 59–70. DOI: 10.1007/s10704-016-0088-8
5. Yuan F., Chen L., Jiang P., Wu X. Twin Boundary Spacing Effects on Shock Response and Spall Behaviors of Hierarchically Nanotwinned FCC Metals. *Journal of Applied Physics*, 2014, Vol. 115, Iss. 6, p. 063509. DOI: 10.1063/1.4865738
6. Kuksin A., Norman G., Stegailov V., Yanilkin A., Zhilyaev P. Dynamic Fracture Kinetics, Influence of Temperature and Microstructure in the Atomistic Model of Aluminum. *International Journal of Fracture*, 2010, Vol. 162, Iss. 1, pp. 127–136. DOI: 10.1007/s10704-009-9424-6
7. Pogorelko V.V., Mayer A.E. Influence of Copper Inclusions on the Strength of Aluminum Matrix at High-Rate Tension. *Materials Science and Engineering: A*, 2015, Vol. 642, pp. 351–359. DOI: 10.1016/j.msea.2015.07.009
8. Pogorelko V.V., Mayer A.E. Influence of Titanium and Magnesium Nanoinclusions on the Strength of Aluminum at High-rate Tension: Molecular Dynamics Simulations. *Materials Science and Engineering: A*, 2016, Vol. 662, pp. 227–240. DOI: 10.1016/j.msea.2016.03.053
9. Krasnikov V.S., Mayer A.E. Plasticity Driven Growth of Nanovoids and Strength of Aluminum at High Rate Tension: Molecular Dynamics Simulations and Continuum Modeling. *International Journal of Plasticity*, 2015, Vol. 74, pp. 75–91. DOI: 10.1016/j.iplas.2015.06.007
10. Kuksin A.Yu., Stegailov V.V., Yanilkin A.V. Atomistic Simulation of Plasticity and Fracture of Nanocrystalline Copper under High-Rate Tension. *Physics Solid State*, 2008, Vol. 50, pp. 2069–2075. DOI: 10.1134/S1063783408110115
11. Stegailov V.V., Yanilkin A.V. Structural Transformations in Single-Crystal Iron During Shock-Wave Compression and Tension: Molecular Dynamics Simulation. *Journal of Experimental and Theoretical Physics*, 2007, Vol. 104, Iss. 6, pp. 928–935. DOI: 10.1134/s1063776107060106
12. Huang L., Han W.Z., An Q., Goddard III W.A., Luo S.N. Shock-Induced Consolidation and Spallation of Cu Nanopowders. *Journal of Applied Physics*, 2012, Vol. 111, Iss. 1, p. 113508. DOI: 10.1063/1.3675174
13. Mackenchery K., Valisetty R.R., Namburu R.R., Stukowski A., Rajendran A.M., Dongare A.M. Dislocation Evolution and Peak Spall Strengths in Single Crystal and Nanocrystalline Cu. *Journal of Applied Physics*, 2016, Vol. 119, Iss. 4, p. 044301. DOI: 10.1063/1.4939867
14. Luo S.N., Germann T.C., Desai T.G., Tonks D.L., An Q. Anisotropic Shock Response of Columnar Nanocrystalline Cu. *Journal of Applied Physics*, 2010, Vol. 107, Iss. 12, p. 123507. DOI: 10.1063/1.3437654
15. Yuan F., Chen L., Jiang P., Wu X. Twin Boundary Spacing Effects on Shock Response and Spall Behaviors of Hierarchically Nanotwinned FCC Metals. *Journal of Applied Physics*, 2014, Vol. 115, Iss. 6, p. 063509. DOI: 10.1063/1.4865738
16. Shao J.L., Wang P., He A., Duan S.Q., Qin C.S. Influence of Voids or He Bubbles on the Spall Damage in Single Crystal Al. *Modelling and Simulation in Materials Science Engineering*, 2014, Vol. 22, no. 2, p. 025012. DOI: 10.1088/0965-0393/22/2/025012
17. Chen Y., Hu H., Tang T., Ren G., Li Q., Wang R., Buttler W.T. Experimental Study of Ejecta from Shock Melted Lead. *Journal of Applied Physics*, 2012, Vol. 111, Iss. 5, p. 053509. DOI: 10.1063/1.3692570
18. Shao J.L., Wang P., He A., Duan S.Q., Qin C.S. Atomistic Simulations of Shock-Induced Microjet from a Grooved Aluminium Surface. *Journal of Applied Physics*, 2013, Vol. 113, Iss. 15, p. 153501. DOI: 10.1063/1.4801800
19. Ren G., Chen Y., Tang T., Li Q. Ejecta Production from Shocked Pb Surface via Molecular Dynamics. *Journal of Applied Physics*, 2014, Vol. 116, Iss. 13, p. 133507. DOI: 10.1063/1.4896902

20. Ebel A.A., Mayer A.E. Influence of Deposited Nanoparticles on the Spall Strength of Metals under the Action of Picosecond Pulses of Shock Compression. *Journal of Physics: Conference Series*, 2018, Vol. 946, P. 012045. DOI: 10.1088/1742-6596/946/1/012045
21. Plimpton S. Fast Parallel Algorithms for Short-Range Molecular Dynamics. *Journal of Computational Physics*, 1995, Vol. 117, Iss. 1, pp. 1–19. DOI: 10.1006/jcph.1995.1039
22. Mishin Y., Farkas D., Mehl M.J., Papaconstantopoulos D.A. Interatomic Potentials for Monoatomic Metals from Experimental Data and *ab initio* calculations. *Physical Review B*, 1999, Vol. 59, Iss. 5, p. 3393–3407.
23. Stukowski A. Visualization and Analysis of Atomistic Simulation Data with OVITO—the Open Visualization Tool. *Modelling and Simulation in Materials Science Engineering*, 2010, Vol. 18, Iss. 1, p. 015012. DOI: 10.1088/0965-0393/18/1/015012
24. Kelchner C.L., Plimpton S.J., Hamilton J.C. Dislocation Nucleation and Defect Structure during Surface Indentation. *Physical Review B*, 1998, Vol. 58, Iss. 17, p. 11085. DOI: 10.1103/physrevb.58.11085
25. Honeycutt J.D., Andersen H.C. Molecular Dynamics Study of Melting and Freezing of Small Lennard-Jones Clusters. *Journal of Physical Chemistry*, 1987, Vol. 91, Iss. 19, pp. 4950–4963. DOI: 10.1021/j100303a014
26. Stukowski A. Structure Identification Methods for Atomistic Simulations of Crystalline Materials. *Modelling and Simulation in Materials Science Engineering*, 2012, Vol. 20, no. 4, p. 045021. DOI: 10.1088/0965-0393/20/4/045021
27. Mayer A.E., Ebel A.A. Influence of Free Surface Nanorelief on the Rear Spallation Threshold: Molecular Dynamics Investigation. *Journal of Applied Physics*, 2016, Vol. 120, Iss. 16, p. 165903. DOI: 10.1063/1.4966555
28. Ebel A.A., Mayer A.E. Molecular Dynamic Investigations of the Shock Pulses Interaction with Nanostructured free Surface of a Target. *Journal of Physics: Conference Series*, 2016, Vol. 774, pp. 012060. DOI: 10.1088/1742-6596/774/1/012060
29. Mayer A.E., Ebel A.A. Shock-Induced Compaction of Nanoparticle Layers into Nanostructured coating. *Journal of Applied Physics*, 2017, Vol. 122, Iss. 16, p. 165901. DOI: 10.1063/1.4996846
30. Subramaniyan A.K., Sun C.T. Continuum Interpretation of Virial Stress in Molecular Simulations. *International Journal of Solids and Structures*, 2008, Vol. 45, Iss. 14–15, pp. 4340–4346. DOI: 10.1016/j.ijsolstr.2008.03.016

Received March 3, 2021

*Bulletin of the South Ural State University
Series "Mathematics. Mechanics. Physics"
2021, vol. 13, no. 2, pp. 53–60*

УДК 538.9

DOI: 10.14529/mmph210208

ЭВОЛЮЦИЯ ПЛАСТИЧЕСКОЙ ДЕФОРМАЦИИ И ТЕМПЕРАТУРЫ ПРИ ОТРАЖЕНИИ УДАРНОГО ИМПУЛЬСА ОТ ПОВЕРХНОСТИ С НАНОРЕЛЬЕФОМ ИЛИ С НАНЕСЕННЫМИ НАНОЧАСТИЦАМИ

А.А. Эбель, А.Е. Майер

Южно-Уральский государственный университет, г. Челябинск, Российская Федерация
E-mail: ebelaa@susu.ru, mayer@csu.ru

Интенсивное облучение и высокоскоростное столкновение металлов приводит к формированию и распространению в них импульсов ударного сжатия. Недавнее развитие экспериментальной техники с использованием мощных субпикосекундных лазерных импульсов позволяет получать ударные импульсы пикосекундного диапазона. В работе проведено молекулярно-динамическое моделирование высокоскоростных столкновений для образцов алюминия. Наличие нанорельефа или осажденных наночастиц на задней поверхности образца может значительно увеличить задний порог расщепления. Взаимодействие ударной волны с нанорельефом или оса-

жденными наночастицами приводит к сильной пластической деформации. В результате часть энергии импульса сжатия расходуется на пластическую деформацию, которая предотвращает разрушение откола. Эффект от повышения порога может достигать сотен метров в секунду по скорости столкновения и десятков гигапаскалей по амплитуде падающей ударной волны. Рассмотрено распределение деформации сдвига и температуры в образце. Показано, что максимальная степень деформации и максимальный нагрев наблюдаются в тех частях нанорельефа, для которых наблюдается наибольшее изменение формы. Максимальная температура достигает точки плавления, но явных следов плавления не обнаружено, что может быть связано со скоростью протекания процессов.

Ключевые слова: высокоскоростное воздействие; пластическая деформация; молекулярная динамика; нанорельеф.

Литература

1. Канель, Г.И. Ударные волны в физике конденсированного состояния / Г.И. Канель, В.Е. Фортов, С.В. Разоренов // УФН. – 2007. – Т. 177, № 8. – С. 809–830.
2. Zaretsky, E.B. Yield Stress, Polymorphic Transformation, and Spall Fracture of Shock-Loaded Iron in Various Structural States and at Various Temperatures / E.B. Zaretsky, G.I. Kanel // Journal of Applied Physics. – 2015. – Vol. 117, Iss. 19. – P. 195901.
3. Механические и оптические свойства ванадия под действием ударных нагрузок пикосекундного диапазона / С.И. Ашитков, П.С. Комаров, Е.В. Струлева и др. // Письма в ЖЭТФ. – 2015. – Т. 101. – Вып. 4. – С. 294–299.
4. Simulation and Experimental Investigation of the Spall Fracture of 304L Stainless Steel Irradiated by a Nanosecond Relativistic High-Current Electron Beam / S.F. Gnyusov, V.P. Rotshtein, A.E. Mayer et al. // International Journal of Fracture. – 2016. – Vol. 199, Iss. 1. – P. 59–70.
5. Yuan, F. Twin Boundary Spacing Effects on Shock Response and Spall Behaviors of Hierarchically Nanotwinned FCC Metals / F. Yuan, L. Chen, P. Jiang, X. Wu // Journal of Applied Physics. – 2014. – Vol. 115, Iss. 6. – P. 063509.
6. Dynamic Fracture Kinetics, Influence of Temperature and Microstructure in the Atomistic Model of Aluminum / A. Kuksin, G. Norman, V. Stegailov et al. // International Journal of Fracture. – 2010. – Vol. 162, Iss. 1. – P. 127–136.
7. Pogorelko, V.V. Influence of Copper Inclusions on the Strength of Aluminum Matrix at High-Rate Tension / V.V. Pogorelko, A.E. Mayer // Materials Science and Engineering: A. – 2015. – Vol. 642. – P. 351–359.
8. Pogorelko, V.V. Influence of Titanium and Magnesium Nano-inclusions on the Strength of Aluminum at High-Rate Tension: Molecular Dynamics Simulations / V.V. Pogorelko, A.E. Mayer // Materials Science and Engineering: A. – 2016. – Vol. 662. – P. 227–240.
9. Krasnikov, V.S. Plasticity Driven Growth of Nanovoids and Strength of Aluminum at High Rate Tension: Molecular Dynamics Simulations and Continuum Modeling / V.S. Krasnikov, A.E. Mayer // International Journal of Plasticity. – 2015. – Vol. 74. – P. 75–91.
10. Kuksin, A.Yu. Atomistic Simulation of Plasticity and Fracture of Nanocrystalline Copper under High-Rate Tension / A.Yu. Kuksin, V.V. Stegailov, A.V. Yanilkin // Physics Solid State. – 2008. – Vol. 50. – P. 2069–2075.
11. Stegailov, V.V. Structural Transformations in Single-Crystal Iron During Shock-Wave Compression and Tension: Molecular Dynamics Simulation / V.V. Stegailov, A.V. Yanilkin // Journal of Experimental and Theoretical Physics. – 2007. – Vol. 104, Iss. 6. – P. 928–935.
12. Shock-induced Consolidation and Spallation of Cu Nanopowders / L. Huang, W.Z. Han, Q. An et al. // Journal of Applied Physics. – 2012. – Vol. 111, Iss. 1. – P. 113508.
13. Dislocation Evolution and Peak Spall Strengths in Single Crystal and Nanocrystalline Cu / K. Mackenberry, R.R. Valisetty, R.R. Namburu et al. // Journal of Applied Physics. – 2016. – Vol. 119, Iss. 4. – P. 044301.
14. Anisotropic Shock Response of Columnar Nanocrystalline Cu / S.N. Luo, T.C. Germann, T.G. Desai et al. // Journal of Applied Physics. – 2010. – Vol. 107, Iss. 12. – P. 123507.
15. Yuan, F. Twin Boundary Spacing Effects on Shock Response and Spall Behaviors of Hierarchically Nanotwinned FCC Metals / F. Yuan, L. Chen, P. Jiang, X. Wu // Journal of Applied Physics. – 2014. – Vol. 115, Iss. 6. – P. 063509.

16. Influence of Voids or He Bubbles on the Spall Damage in Single Crystal Al / J.L. Shao, P. Wang, A. He *et al.* // *Modelling and Simulation in Materials Science Engineering*. – 2014. – Vol. 22, no. 2. – P. 025012.
17. Chen, Y. Experimental Study of Ejecta from Shock Melted Lead / Y. Chen, H. Hu, T. Tang *et al.* // *Journal of Applied Physics*. – 2012. – Vol. 111, Iss. 5. – P. 053509.
18. Atomistic simulations of shock-induced microjet from a grooved aluminium surface / J.L. Shao, P. Wang, A. He *et al.* // *Journal of Applied Physics*. – 2013. – Vol. 113, Iss. 15. – P. 153501.
19. Ejecta Production from Shocked Pb Surface via Molecular Dynamics / G. Ren, Y. Chen, T. Tang, Q. Li // *Journal of Applied Physics*. – 2014. – Vol. 116, Iss. 13. – P. 133507.
20. Ebel, A.A. Influence of Deposited Nanoparticles on the Spall Strength of Metals under the Action of Picosecond Pulses of Shock Compression / A.A. Ebel, A.E. Mayer // *Journal of Physics: Conference Series*. – 2018. – Vol. 946. – P. 012045.
21. Plimpton, S. Fast Parallel Algorithms for Short-Range Molecular Dynamics. *Journal of Computational Physics*, 1995, Vol. 117, Iss. 1, pp. 1–19. DOI: 10.1006/jcph.1995.1039
22. Mishin, Y. Interatomic Potentials for Monoatomic Metals from Experimental Data and Ab Initio Calculations / Y. Mishin, D. Farkas, M.J. Mehl, D.A. Papaconstantopoulos // *Physical Review B*. – 1999. – Vol. 59, Iss. 5. – P. 3393–3407.
23. Stukowski, A. Visualization and Analysis of Atomistic Simulation Data with OVITO—the Open Visualization Tool / A. Stukowski // *Modelling and Simulation in Materials Science Engineering*. – 2010. – Vol. 18. – P. 015012.
24. Kelchner, C.L. Dislocation Nucleation and Defect Structure During Surface Indentation / C.L. Kelchner, S.J. Plimpton, J.C. Hamilton // *Physical Review B*. – 1998. – Vol. 58, Iss. 17. – P. 11085.
25. Honeycutt, J.D. Molecular Dynamics Study of Melting and Freezing of Small Lennard-Jones Clusters / J.D. Honeycutt, H.C. Andersen // *Journal of Physical Chemistry*. – 1987. – Vol. 91, Iss. 19. – P. 4950–4963.
26. Stukowski, A. Structure Identification Methods for Atomistic Simulations of Crystalline Materials / A. Stukowski // *Modelling and Simulation in Materials Science Engineering*. – 2012. – Vol. 20, no. 4. – P. 045021.
27. Mayer, A.E. Influence of Free Surface Nanorelief on the Rear Spallation Threshold: Molecular Dynamics Investigation / A.E. Mayer, A.A. Ebel // *Journal of Applied Physics*. – 2016. – Vol. 120, Iss. 16. – P. 165903.
28. Ebel, A.A. Molecular Dynamic Investigations of the Shock Pulses Interaction with Nanostructured Free Surface of a Target / A.A. Ebel, A.E. Mayer // *Journal of Physics: Conference Series*. – 2016. – Vol. 774. – P. 012060.
29. Mayer, A.E. Shock-Induced Compaction of Nanoparticle Layers into Nanostructured Coating / A.E. Mayer, A.A. Ebel // *Journal of Applied Physics*. – 2017. – Vol. 122, Iss. 16. – P. 165901.
30. Subramaniyan, A.K. Continuum Interpretation of Virial Stress in Molecular Simulations / A.K. Subramaniyan, C.T. Sun // *International Journal of Solids and Structures*. – 2008. – Vol. 45, Iss. 14–15. – P. 4340–4346.

Поступила в редакцию 3 марта 2021 г.